Plasma Membrane Fusion Is Specifically Impacted by the Molecular Structure of Membrane Sterols During Vegetative Development of *Neurospora crassa*

Martin Weichert,*,[1] Stephanie Herzog,*,[1] Sarah-Anne Robson,* Raphael Brandt,*,[2] Bert-Ewald Priegnitz,* Ulrike Brandt,* Stefan Schulz,† and André Fleißner*,[3]

*Institut für Genetik, Technische Universität Braunschweig, 38106 Braunschweig, Germany and †Institut für Organische Chemie, Technische Universität Braunschweig, 38106 Braunschweig, Germany

ORCID ID: 0000-0002-7484-9520 (M.W.)

ABSTRACT Cell-to-cell fusion is crucial for the development and propagation of most eukaryotic organisms. Despite this importance, the molecular mechanisms mediating this process are only poorly understood in biological systems. In particular, the step of plasma membrane merger and the contributing proteins and physicochemical factors remain mostly unknown. Earlier studies provided the first evidence of a role of membrane sterols in cell-to-cell fusion. By characterizing different ergosterol biosynthesis mutants of the fungus *Neurospora crassa*, which accumulate different ergosterol precursors, we show that the structure of the sterol ring system specifically affects plasma membrane merger during the fusion of vegetative spore germlings. Genetic analyses pinpoint this defect to an event prior to engagement of the fusion machinery. Strikingly, this effect is not observed during sexual fusion, suggesting that the specific sterol precursors do not generally block membrane merger, but rather impair subcellular processes exclusively mediating fusion of vegetative cells. At a colony-wide level, the altered structure of the sterol ring system affects a subset of differentiation processes, including vegetative sporulation and steps before and after fertilization during sexual propagation. Together, these observations corroborate the notion that the accumulation of particular sterol precursors has very specific effects on defined cellular processes rather than nonspecifically disturbing membrane functioning. Given the phenotypic similarities of the ergosterol biosynthesis mutants of *N. crassa* during vegetative fusion and of *Saccharomyces cerevisiae* cells undergoing mating, our data support the idea that yeast mating is evolutionarily and mechanistically more closely related to vegetative than sexual fusion of filamentous fungi.

KEYWORDS ergosterol; cell fusion; plasma membrane fusion; mating; *Neurospora crassa*

Fusion between genetically and developmentally identical or different cells is a common process in the growth and development, of eukaryotic organisms. It serves a plethora of biological functions including gamete merger during sexual propagation, muscle and organ development, neuronal repair, or the formation of multinucleate cells, such as macrophage-derived osteoclasts or giant cells. In filamentous fungi, cell-to-cell fusion promotes multicellular growth and the formation and functioning of mycelial colonies. In many ascomycete species, the cell tips of germinating vegetative spores (conidia) mutually attract each other during colony establishment and fuse into supracellular networks (germling fusion) that further develop into the hyphal colony (Roca *et al.* 2005). This cooperation of genetically identical individuals likely promotes competitiveness and allows the coordinated conquering of a specific habitat by clonal spores (Richard *et al.* 2012). Within mature mycelial colonies, fusion between hyphal branches (hyphal fusion) increases the interconnectivity within the cellular network, promoting the exchange of water and nutrients throughout the colony, and supporting its coordinated growth and propagation.

In addition, the sexual reproduction of outcrossing fungal species involves the merger of two genetically different mating partners. Fertilization is typically achieved through the fusion of specialized reproduction structures or cells to enable

Copyright © 2020 by the Genetics Society of America
doi: https://doi.org/10.1534/genetics.120.303623
Manuscript received August 21, 2020; accepted for publication October 11, 2020; published Early Online October 12, 2020.
Supplemental material available at figshare: https://doi.org/10.25386/genetics.13050176.
[1]These authors contributed equally to this work.
[2]Present address: Institute for Functional Anatomy, Charité – Universitätsmedizin Berlin, 10117 Berlin, Germany.
[3]Corresponding author: Biozentrum/Room 357, Technische Universität Braunschweig, Spielmannstrasse 7, 38106 Braunschweig, Germany. E-mail: a.fleissner@tu-bs.de

subsequent nuclear fusion and genetic recombination (Bistis 1981).

Despite the broad occurrence and high relevance of cell-to-cell fusion, the molecular mechanisms mediating this process remain only poorly understood in any biological system. In particular, the last step of the cell-to-cell fusion process, the merger of the plasma membranes, remains enigmatic. In recent years, the red bread mold *Neurospora crassa* has advanced as a model system for studying the molecular mechanisms of eukaryotic cell-to-cell fusion in general, and fungal colony initiation and development in particular (Herzog *et al.* 2015; Fischer and Glass 2019). In vegetative germling fusion, *N. crassa* employs an unusual communication mechanism, in which the two fusion partners take turns in signal sending and receiving. As a result of this cellular dialog, the germlings direct their growth toward each other until physical contact is achieved (Fleissner *et al.* 2009a; Fleißner and Herzog 2016). While the molecular factors governing these cellular interactions are starting to unfold, the mechanisms mediating the fusion process after cell-to-cell contact remain mostly elusive. Fusion pore formation requires cell wall remodeling, followed by adherence and subsequent fusion of the plasma membranes. So far, no *bona fide* fusogen, a protein required and sufficient for plasma membrane merger, has been identified in fungi (Aguilar *et al.* 2013). However, transmembrane proteins promoting plasma membrane fusion during vegetative and sexual cell merger have been described in *Saccharomyces cerevisiae*, *Schizosaccharomyces pombe*, and *N. crassa*. In all species, a significant fraction of fusion pairs lacking the PRM1 protein fail to merge the plasma membranes and remain with tightly adhered lipid bilayers (Heiman and Walter 2000; Fleissner *et al.* 2009b; Curto *et al.* 2014). A similar but less-severe defect is observed in Δ*lfd-1* mutants of *N. crassa*, in which about one-fifth of fusion pairs fail in membrane merger (Palma-Guerrero *et al.* 2014). PRM1 and LFD-1 mediate both vegetative and sexual fusion, suggesting that both are part of a general fusion machinery. In addition to the membrane merger defect, all of the described *S. cerevisiae* and *N. crassa* mutants exhibit significantly increased lysis of fusion pairs. The onset of lysis coincides with the moment of cytoplasmic mixture, suggesting that it is caused by the engagement but aberrant functioning of the fusion machinery (Aguilar *et al.* 2007; Palma-Guerrero *et al.* 2014).

In addition to fusion-mediating proteins, plasma membrane merger is also influenced by the composition of the lipid bilayer itself. Crucial lipid constituents of eukaryotic cell membranes are sterols, which have essential roles for membrane properties and the functioning of membrane-associated proteins (Dufourc 2008). Different *S. cerevisiae* and *N. crassa* mutants deficient in the biosynthesis of ergosterol, the prevalent sterol in fungal cell membranes, are affected in cell fusion-related cellular communication or plasma membrane merger (Jin *et al.* 2008; Aguilar *et al.* 2010; Weichert *et al.* 2016). Strikingly, specific phenotypic deficiencies of some ergosterol biosynthesis (*erg*) mutants correlate with specific structural features of the accumulating sterol precursors. For example, a defect in the last step of ergosterol biosynthesis mediated by the sterol C-24(28) reductase ERG-2 results in the accumulation of a precursor carrying a conjugated double bond in its aliphatic side chain. As a consequence, signaling through the MAK-1 mitogen-activated protein kinase (MAPK) cascade, which is essential for germling communication and cell-to-cell contact recognition in *N. crassa*, is strongly affected, while other related membrane-associated signaling processes, including a second MAPK pathway (MAK-2), remain functional (Weichert *et al.* 2016). These observations indicate that changes in the sterol structure have specific rather than general effects on cell functioning.

In *S. cerevisiae*, mutants accumulating ergosterol precursors with an altered double-bond configuration in the B ring (Δ*erg2* or Δ*erg3*, Figure 1A) exhibit a Δ*prm1*-like phenotype, with a significant percentage of mating pairs remaining in the stage of closely adhered plasma membranes. Despite the morphological similarities of the Δ*prm1* and *erg* mutants, both defects act independently, indicated by additive effects in the respective double mutants (Jin *et al.* 2008). However, so far the molecular processes affected by the accumulation of intermediates of ergosterol biosynthesis in these *erg* mutants remain unknown.

Here, we show that structural changes in the ring system of ergosterol lead to membrane fusion deficiencies during vegetative cell-to-cell fusion in *N. crassa*, indicating functional conservation between yeast mating and vegetative fusion in the filamentous fungus. However, sexual cell-to-cell merger remains unaffected in the *erg* mutants of *N. crassa*, indicating that the altered membrane structure does not compromise the general basic fusion machinery. Consistent with these findings, we could pinpoint the sterol-dependent defect in plasma membrane merger to a step prior to the engagement of the fusion machinery, suggesting a novel role of membrane structure in the signaling events preceding the initiation of plasma membrane fusion.

Materials and Methods

Strains and growth conditions

The strains of *N. crassa* used and generated in this study are listed in Supplemental Material, Table S1. Strains were routinely grown at 30° in agar slant tubes containing Vogel's minimal medium (MM) (Vogel 1956) as previously described in Schürg *et al.* (2012). Crosses were conducted on Westergaard's medium (Westergaard and Mitchell 1947) as described before (Serrano *et al.* 2018). Spores were obtained from 1-week-old cultures through harvesting in sterile distilled water. Spore suspensions were filtered through Miracloth (Calbiochem, San Diego, CA) and counted with a hemocytometer.

Linear hyphal growth rates were determined as described in Fleissner *et al.* (2005). To quantify sporulation, the strains were first grown in MM slant tubes for 7 days at 26° with a

12-hr light–dark rhythm. Conidia were harvested in 2 ml of sterile distilled water and purified from hyphal fragments by filtration through Miracloth. The spore numbers per tube were determined with a hemocytometer. To determine the lengths of aerial hyphae, 2 ml of liquid MM in a long reaction tube inoculated with 10^4 spores were incubated for 5 days at 30° in the dark.

To compare the sensitivity of strains to nystatin, agar plates with sorbose-rich medium, which induces colonial growth in *N. crassa* (Tatum *et al.* 1949), were spotted with 5-μl droplets of 10-fold serial dilutions of spore suspensions, resulting in 10^5–10 conidia per spot. The media were supplemented with freshly prepared solutions of nystatin dihydrate (100 μg/ml in DMSO; Roth). Photos of the plates were captured after incubation at 30° for 72 hr.

Strain construction

Complementation of Δerg-10a/Δerg-10b: To complement the double mutant Δ*erg-10a*/Δ*erg-10b*, strain MW_126 was transformed with plasmids containing either the gene *erg-10a* (NCU06207) or *erg-10b* (NCU04983), including 1000 bp upstream and downstream of these sequences. To construct the plasmids, both genes were PCR-amplified from genomic DNA of the wild-type (WT) strain FGSC (Fungal Genetics Stock Center) 2489 using the primer pairs 1445/1446 and 1447/1448, respectively (Table S2). The PCR products were cloned via PacI and NotI into vector 728 (a pMF272 [Freitag *et al.* 2004] derivative lacking the *gfp* sequence), enabling the site-specific integration at the *his-3* locus of the *N. crassa* genome (Freitag and Selker 2005). The resulting plasmids 745 (*erg-10a*) and 746 (*erg-10b*) were transformed into the histidine-auxotrophic double mutant MW_126 as described in Margolin *et al.* (1997).

Construction of erg-1 gene deletion strains: For the deletion of *erg-1* in *N. crassa*, a gene replacement cassette for homologous recombination was constructed using yeast recombinational cloning (Raymond *et al.* 1999) as described in Colot *et al.* (2006). The 5′ and 3′ untranslated regions of the *erg-1* gene were PCR-amplified from genomic DNA of strain FGSC 9719 with primer pairs 103/104 and 105/106, respectively (Table S2). Using the *S. cerevisiae* strain FY834 for the yeast transformation (Winston *et al.* 1995), these flanks were assembled with the hygromycin resistance gene amplified with primers 82/83 from plasmid pCSN44 (Staben *et al.* 1989) and the EcoRI/XhoI-linearized yeast vector pRS426 (Christianson *et al.* 1992) as described before (Colot *et al.* 2006). The plasmid DNA extracted from the yeast colonies was used as a template in a PCR with primers 103 and 106 to amplify the assembled *erg-1* gene deletion cassette. Transformation of *N. crassa* with the gene knockout cassette was performed as previously described (Fleissner and Glass 2007), using the *mus-52*::*bar* deletion mutant FGSC 9719 as the recipient strain for efficient homologous recombination (Colot *et al.* 2006). Transformants were confirmed by Southern blot analysis and purified by backcrossing with the WT strain. To generate Δ*erg-1* strains expressing cytosolic GFP and mCherry, a mutant auxotrophic for histidine (MW_347) was transformed with plasmids pMF272 (Freitag *et al.* 2004) and pMFcherry (Schürg *et al.* 2012), respectively. Accordingly, a histidine-auxotrophic double deletion strain lacking both *erg-1* and *Prm1* (MW_450) was transformed in the same way to generate Δ*Prm1*/Δ*erg-1* strains expressing GFP and mCherry, respectively.

Construction of erg mutants lacking Prm1: Mutants lacking *erg* genes and *Prm1* were obtained via sexual crosses (data not shown). The strains lacking *erg-10a*, *erg-10b*, and *Prm1*, and expressing cytosolic GFP and mCherry, respectively, were constructed by transforming a histidine-auxotrophic triple mutant (MW_277.1) with the vectors pMF272 or pMFcherry.

Cell-to-cell fusion assays

Vegetative spore germling fusion assays were conducted as previously described (Fleissner *et al.* 2009b). In brief, conidial suspensions were spread on MM agar plates, incubated at 30° for 4 hr and analyzed by brightfield and fluorescence microscopy. Agar blocks of ∼10 × 10 mm were cut from the plates, covered with coverslips, and analyzed by brightfield and fluorescence microscopy. The number of germlings undergoing directed growth toward each other was determined from microscopic images with comparable cell densities as previously described (Weichert *et al.* 2016). The quantitative analysis of cell-to-cell fusion between germlings expressing green- and red-fluorescing proteins was performed as described in Fleissner *et al.* (2009b). For live-cell imaging of SO-GFP and MAK-2-GFP in interacting germlings, samples were prepared as described above and analyzed by fluorescence microscopy (Fleissner *et al.* 2009a). Sexual fusion between trichogynes and microconidia was assessed as described in Fleissner *et al.* (2005).

Analysis of fruiting body development

The phenotypic characterization of fruiting bodies and progeny was performed with a stereomicroscope as described in Weichert *et al.* (2016). To determine the number of protoperithecia per area unit, strains were grown on crossing plates for 7 days as described above. The quantification of the protoperithecia was based on representative images captured from at least three independent cultures. The average number of protoperithecia per 1 mm^2 was determined using the software Fiji (https://fiji.sc/). Images of perithecia were taken 10–14 days after fertilization, either as viewed from above the crossing plates or at an angle of ∼45° relative to the camera. Rosettes of asci from crosses were prepared by placing isolated perithecia into a droplet of water on a glass slide and gently squeezing them under a coverslip. At least 1 month after fertilization, ejected ascospores were harvested in 2 ml of sterile distilled water from the lids of the crossing plates, heat-activated at 59° for 20 min, spread on MM plates, and incubated at room temperature for 16–20 hr. Germinating ascospores were analyzed with a stereomicroscope and isolated in MM slant tubes for growth into vegetative mycelia.

Staining of the plasma membrane and cell wall of germling pairs

The staining of cell membranes with FM4-64 was performed as described in Hickey *et al.* (2002). FM4-64 was prepared as a solution of 100 μg in 1 ml of sterile distilled water, which was further diluted to working solutions of 25 μM.

To simultaneously stain the cell membrane and the cell wall in germling pairs, samples were treated with 10 μl of a mixture of FM4-64 and calcofluor white (CFW, fluorescence brightener 28). First, CFW was prepared as a stock solution of 7 mg/ml in DMSO and then diluted 1:100 in sterile distilled water. Next, one volume of the working solution of CFW was mixed with nine volumes of the working solution of FM4-64, which were immediately used for fluorescence microscopy of the double-stained germling pairs.

Analysis of cell lysis in germling pairs

Fusion-induced cell lysis was quantified as previously described in Schumann *et al.* (2019), using MM with normal and reduced Ca^{2+} concentrations (0.68 and 0.34 mM, respectively).

Visualization of sterol distribution in germlings and trichogynes

To determine the distribution of plasma membrane sterols in interacting germlings, samples were prepared as described above and treated with 10 μl containing 100 μg/ml of filipin III (Sigma [Sigma-Aldrich], St. Louis, MO) in 1% (v/v) DMSO. Trichogynes were obtained from crosses as described in Fleissner *et al.* (2005), followed by the treatment of samples (agar blocks of 5 × 5 mm) with 5 μl of the filipin III solution between 24 and 48 hr after incubation. Cells were analyzed within 15 min after filipin staining by fluorescence microscopy using a DAPI filter setup.

Brightfield and fluorescence microscopy

Images of germlings were captured with an Axiophot 2 microscope (Zeiss [Carl Zeiss], Jena, Germany) coupled to a pixelfly 270 XS (pco) camera, using 63×/1,40 oil plan-apochromat and 100×/1,30 oil plan-neofluar objectives and DIC optics. The double-staining of germlings with FM4-64 and CFW was performed using an Axio Observer.Z1 inverse microscope (Zeiss) using light-emitting diodes for the excitation light. Brightfield images of fruiting bodies and asci were captured with an M60 stereomicroscope (Leica) coupled to a DFC295 camera.

Sterol extraction and analysis

The extraction and analysis of sterols was performed as described in our previous study (Weichert *et al.* 2016). In brief, sterols were isolated from frozen, ground mycelia using a 3:1 (v/v) mixture of chloroform and methanol, subsequent saponification with 10% (w/v) potassium hydroxide in methanol, followed by extraction in *n*-hexane. Sterol extracts were derivatized with 2,2,2-trifluoro-*N*-methyl-*N*-(trimethylsilyl) acetamide and analyzed by gas chromatography/mass spectrometry (GC/MS) as described in (Nawrath *et al.* 2010). The sterol biosynthesis intermediates were identified by comparing their mass spectra with data available from databases and the literature.

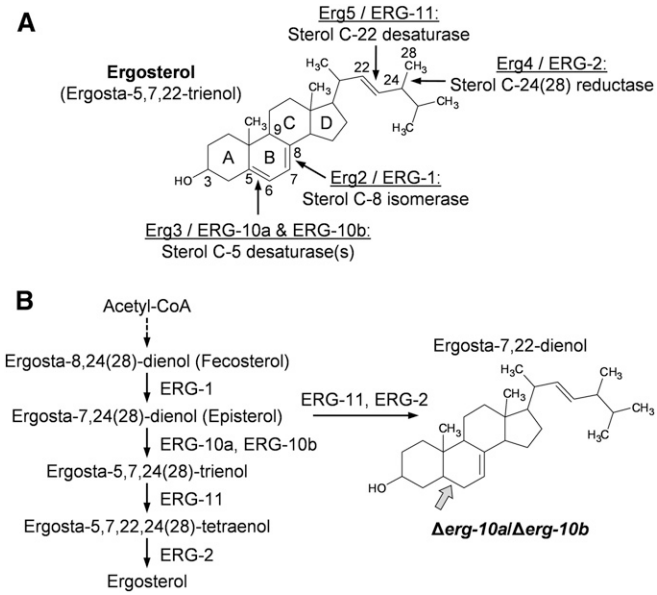

Figure 1 The sterol C-5 desaturases ERG-10a and ERG-10b have a redundant function in ergosterol biosynthesis in *N. crassa*. (A) Structure of ergosterol. Enzymes and their functions mediating double-bond arrangements in ergosterol precursors are depicted (*S. cerevisiae*/*N. crassa*). Numbers along ergosterol denote the position of selected carbon atoms, and letters indicate the carbon rings. (B) Late steps in the hypothetical biosynthesis pathway of ergosterol in *N. crassa* showing the reactions catalyzed by the enzymes presented in (A). ERG-10a and ERG-10b mediate the same reaction, whose block results in the accumulation of a sterol intermediate with an altered ring structure (gray arrow).

Statistical analysis

Statistical data analysis was performed with GraphPad Prism (version 8.3.1) using analysis of variance (ANOVA) with Tukey's or Dunnett's multiple comparison tests, or unpaired, two-tailed Student's *t*-tests, to evaluate statistically significant differences in fungal growth, cell-to-cell fusion, and cell lysis.

Data availability

Strains and plasmids are available upon request. The authors affirm that all reagents, software, and data that are necessary for drawing the conclusions presented in this study are fully represented within this article, and its tables and figures. Supplemental material available at figshare: https://doi.org/10.25386/genetics.13050176.

Results

The absence of the redundant sterol C-5 desaturases ERG-10a and ERG-10b affects specific differentiation steps in the life cycle of N. crassa

In earlier studies, we reported that the sterol C-5 desaturases ERG-10a and ERG-10b, encoded by the gene loci NCU06207

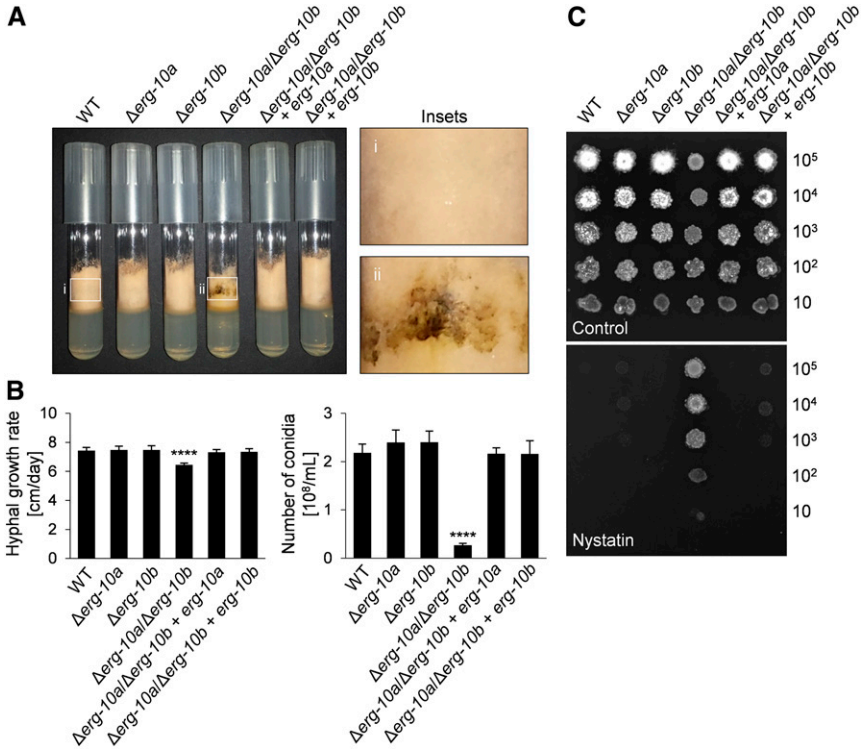

Figure 2 Impact of Δ*erg-10a* and Δ*erg-10b* on vegetative growth of *N. crassa*. (A) Growth of WT (FGSC 2489), Δ*erg-10a* (FGSC 20057), Δ*erg-10b* (N4-30), Δ*erg-10a*/Δ*erg-10b* (N4-38), Δ*erg-10a*/Δ*erg-10b* + *erg-10a* (MW_630), and Δ*erg-10a*/Δ*erg-10b* + *erg-10b* (MW_631) in MM tubes. Insets: in contrast to WT (i), Δ*erg-10a*/Δ*erg-10b* (ii) typically produces dark pigments along the glass wall of the tube. (B) Quantification of linear hyphal extension rates and sporulation. Values represent the mean ± SD from at least three independent experiments per strain (****$P < 0.0001$, ANOVA with Tukey's *post hoc* test). (C) Ten-fold serial dilutions of conidia of the indicated strains were spotted onto sorbose-rich medium in the absence or presence of the polyene antifungal compound nystatin. FGSC, Fungal Genetics Stock Center; MM, minimal medium; WT, wild-type.

and NCU04983, respectively, have a redundant function in ergosterol biosynthesis in *N. crassa* (Weichert *et al.* 2016; Herzog *et al.* 2020). They introduce a double bond between C-5 and C-6 of the B ring in the sterol molecule (Figure 1A). Their absence results in the accumulation of ergosta-7,22-dienol, which differs from ergosterol only by the lack of this specific double bond (Figure 1B).

To test if this metabolic defect influences growth and development of the fungus, we characterized respective gene knockout mutants. Consistent with the redundant function of ERG-10a and ERG-10b, mutants lacking the individual genes (FGSC 20057 and N4-30, respectively) were macroscopically indistinguishable from the WT reference strain FGSC 2489 (Figure 2A). However, a Δ*erg-10a*/Δ*erg-10b* double mutant (N4-38) showed a strong decrease in asexual spore differentiation, whereas the overall growth rate was only slightly affected (Figure 2B) and aerial hyphae formation was WT-like (data not shown). In contrast to the WT or single mutants, cultures of the double mutant also accumulated a brownish pigment (Figure 2A). Reintegration of either the *erg-10a* or *erg-10b* gene into the double mutant restored the WT phenotype, confirming the redundant functions of the encoded enzymes (Figure 2, A and B).

Due to their lack of ergosterol, classical *erg* mutants of *N. crassa* generated by UV mutagenesis show increased resistance to ergosterol-binding antifungals called polyenes (Grindle 1973, 1974). The Δ*erg-10a*/Δ*erg-10b* isolate was also less sensitive to the polyene nystatin than the WT, the single-gene deletion mutants, or the complemented strains (Figure 2C), consistent with a block in ergosterol biosynthesis in the double mutant. Taken together, the presence of either ERG-10a or ERG-10b sufficiently supports WT-like growth of *N. crassa*, while the absence of both sterol C-5 desaturases results in a specific deficiency in spore differentiation.

The lack of ERG-10a and ERG-10b results in plasma membrane fusion deficiencies during vegetative germling fusion

Our earlier study revealed that Δ*erg-2* germlings interact at a significantly reduced frequency and are unable to arrest growth after cell-to-cell contact. In contrast, directed growth of Δ*erg-10a*/Δ*erg-10b* germlings is comparable to WT (Weichert *et al.* 2016). The interaction of WT germlings includes membrane recruitment of the MAPK MAK-2 and the fungal-specific signaling factor SO (Fleissner *et al.* 2009a). As expected, the membrane recruitment of both proteins was also unaffected in the Δ*erg-10a*/Δ*erg-10b* double mutant (Figure S1). The structural differences of ergosta-7,22-dienol and ergosterol therefore have no effect on the membrane-associated signaling processes preceding cell-to-cell contact, in contrast to the changed aliphatic side chain of the sterol accumulating in Δ*erg-2*.

To test for potential fusion defects after cell-to-cell contact, germlings from WT or Δ*erg-10a*/Δ*erg-10b* strains expressing either cytosolic GFP or mCherry were mixed, and incubated to allow cell-to-cell interactions. Cell pairs consisting of a red and a green cell were analyzed by fluorescence microscopy. WT cell pairs mostly exhibited both fluorescent markers in either fusion partner, indicating cytoplasmic mixing as a result of cell-to-cell fusion (Figure 3A). In contrast, >30% of

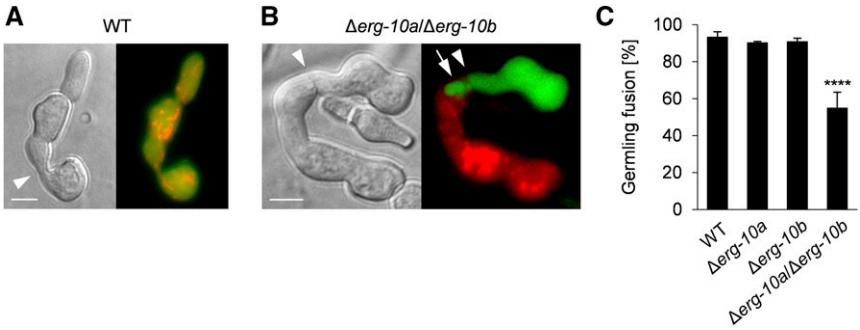

Figure 3 Germlings of Δ*erg-10a*/Δ*erg-10b* are impaired in cell-to-cell fusion. (A) Microscopic analysis of cell-to-cell fusion in a pair of WT germlings expressing cytosolic GFP and Cherry Red (N3-06 + N3-07) after physical contact (arrowhead), resulting in mixing of green and red fluorescence. (B) A pair of Δ*erg-10a*/Δ*erg-10b* germlings expressing cytosolic GFP or Cherry Red (MW_175 + MW_179). Note the lack of cytoplasmic mixing and the extrusion extending from one cell into the other (arrow). Bar in (A and B), 5 μm. (C) Quantification of germling fusion in cell pairings of WT (N3-06 + N3-07), Δ*erg-10a* (N5-01 + N5-02), Δ*erg-10b* (MW_103 + MW_105), and Δ*erg-10a*/Δ*erg-10b* (MW_175 + MW_179). Values represent the mean ± SD from at least three independent cell populations with 87–109 germling pairs per replicate (****$P < 0.0001$, ANOVA with Tukey's *post hoc* test). WT, wild-type.

Δ*erg-10a*/Δ*erg-10b* pairs failed to exchange their cytoplasm, although the cells were tightly adhered to one another (Figure 3, B and C). We also analyzed the Δ*erg-11* and Δ*erg-2*/Δ*erg-11* mutants, which interact in a WT-like manner (Weichert *et al.* 2016). These isolates were not affected in their fusion frequencies (88.2 ± 0.8% and 87.4 ± 1.5%, respectively), indicating that the Δ*erg-10a*/Δ*erg-10b* fusion deficiency represents a novel phenotype among all of the *erg* mutants of *N. crassa* tested so far.

In nonfused Δ*erg-10a*/Δ*erg-10b* cell pairs, one cell often formed a finger-like structure, which reached into the cytoplasm of the opposing cell (Figure 3B). This phenotype strongly resembled the earlier reported membrane fusion defect of *S. cerevisiae* or *N. crassa* Δ*prm1* mutants. In both species, 50% of mutant cell pairs fail to merge their tightly opposed plasma membranes after successful cell wall deconstruction (Heiman and Walter 2000; Fleissner *et al.* 2009b). The comparison of green- and red-fluorescing cell pairs of Δ*erg-10a*/Δ*erg-10b* and Δ*Prm1* readily revealed comparable finger- or bubble-like structures in both mutants (Figure S2). This striking phenotypic similarity suggested that the Δ*erg-10a*/Δ*erg-10b* mutant is also defective in plasma membrane merger after cell wall remodeling. Costaining of the cell wall and the plasma membrane confirmed that unfused Δ*Prm1* and Δ*erg-10a*/Δ*erg-10b* germling pairs both showed a WT-like opening in the cell wall, but no subsequent fusion pore formation (Figure 4A). Complementation of the double mutant with either the *erg-10a* or *erg-10b* gene fully restored WT-like fusion pore formation (Figure S3). These observations indicate that the altered sterol composition in the Δ*erg-10a*/Δ*erg-10b* mutant specifically affects plasma membrane fusion after cell wall degradation.

The germling fusion defects of Δerg-10a/Δerg-10b are independent of PRM1 and LFD-1

The striking resemblance of the membrane fusion defects of the Δ*Prm1* and Δ*erg-10a*/Δ*erg-10b* mutants suggested that accumulation of the ergosterol precursor could specifically impair the function of the PRM1 protein. To test this hypothesis, we employed classical genetics and analyzed membrane fusion in a Δ*Prm1*/Δ*erg-10a*/Δ*erg-10b* triple mutant. As expected, the deletion of all three genes also caused membrane invaginations similar to those found in cell pairs of Δ*Prm1* or Δ*erg-10a*/Δ*erg-10b* (Figure S2). However, the rate of successful fusion dropped in the triple mutant to <10% compared with ~50% and 60% in Δ*Prm1* and Δ*erg-10a*/Δ*erg-10b*, respectively (Figure 4B). These data indicate that the fusion defects of Δ*Prm1* and Δ*erg-10a*/Δ*erg-10b* are independent, suggesting that the altered sterol composition of this *erg* mutant does not impact PRM1 functions.

To further investigate this question, we quantified fusion in heterotypic germling pairs. Consistent with previous observations (Heiman and Walter 2000; Fleissner *et al.* 2009b), the fusion frequencies of Δ*Prm1* and Δ*erg-10a*/Δ*erg-10b* cells approached almost normal levels (~85%) when one of the interaction partners was WT (Figure 4B). Similarly, mixed germling pairs consisting of a Δ*erg-10a*/Δ*erg-10b* and a Δ*Prm1* cell exhibited 80% fusion success, indicating that the mutants can mutually compensate their deficiencies.

In *N. crassa*, the LFD-1 protein possesses a redundant role that is independent of PRM1 during plasma membrane merger (Palma-Guerrero *et al.* 2014). Consistent with these earlier studies, we also observed the formation of membrane invaginations after cell-to-cell contact with a relatively mild effect on membrane fusion in a Δ*lfd-1* mutant (Figure S4, A–C). A triple mutant lacking *lfd-1*, *erg-10a*, and *erg-10b* showed slightly further reduced fusion frequencies compared to Δ*erg-10a*/Δ*erg-10b* (Figure S4C). These observations suggest that LFD-1 is rather a supporting factor during plasma membrane merger that, similarly to PRM1, acts independently of the altered sterol composition of Δ*erg-10a*/Δ*erg-10b*.

Structural alterations in the sterol ring system in the Δerg-1 mutant also disturb plasma membrane fusion between germlings

Our earlier study revealed that the structural features of the main sterol accumulating in *erg* mutants can very specifically correlate with distinct developmental and cell biological defects (Weichert *et al.* 2016). Since the membrane fusion defect of Δ*erg-10a*/Δ*erg-10b* germlings was unique among all of the *N. crassa* ergosterol biosynthesis mutants tested so far, we

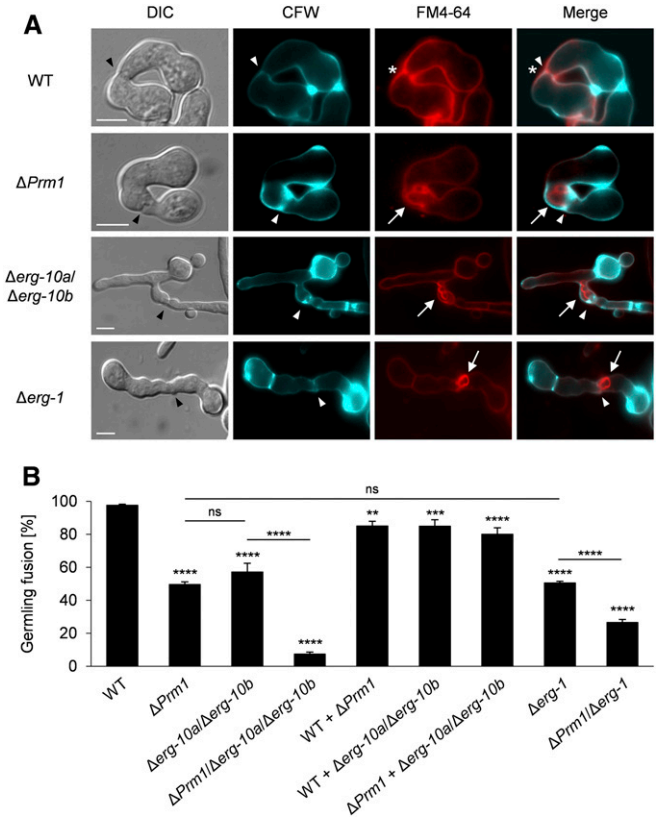

Figure 4 Germlings of the mutants Δ*erg-10a* Δ*erg-10b* and Δ*erg-1* are defective in plasma membrane merger during cell-to-cell fusion. (A) Costaining with CFW and FM4-64 to visualize the cell wall and the plasma membrane, respectively. Black arrowheads indicate cell contacts. Note that WT (FGSC 2489) pairings form both an opening in the cell wall (white arrowhead) and a fusion pore in the membrane (asterisk). The mutants Δ*Prm1* (A32), Δ*erg-10a*/Δ*erg-10b* (N4-38), and Δ*erg-1* (MW_308) form membrane invaginations (arrows) that stretch through the cell wall opening from one into the other cell (white arrowheads). Bar, 5 μm. (B) Quantification of germling fusion of *erg* mutants carrying the additional deletion of *Prm1*. Values represent the mean ± SD from three independent experiments per set of strains with a range of 40–211 germling pairs per population (**$P < 0.01$, ***$P < 0.001$, ****$P < 0.0001$; ANOVA with Tukey's *post hoc* test). See Figure S2 for images of representative germling pairs from these experiments. CFW, calcofluor white; ns, not significant; WT, wild-type.

hypothesized that this phenotype correlates with specific structural features of the sterol precursor formed by this mutant. Of all previously described *erg* mutants, Δ*erg-10a*/Δ*erg-10b* is the only one to accumulate ergosta-7,22-dienol (Weichert *et al.* 2016), which differs from ergosterol only by a missing double bond in the ring system (Figure 1, A and B). Therefore, we decided to analyze mutants of the gene *erg-1* (NCU04156), which encodes a sterol C-8 isomerase homologous to Erg2 of *S. cerevisiae*, that contributes to the structure of the sterol ring system (Figure 1A). Earlier studies indicated that a classical *erg-1* mutant obtained by random mutagenesis (FGSC 2721) accumulates sterols with a double bond between positions C-8 and C-9, instead of C-7 and C-8 (Grindle 1973, 1974; Grindle and Farrow 1978). We confirmed this mutant by sequencing of the *erg-1* gene, which revealed a single point mutation that results in a Gly to Asp substitution at position 66 of the protein. Interestingly, the macroscopic appearance of the *erg-1* mutant resembled the Δ*erg-10a*/Δ*erg-10b* strain, including the characteristic pigment production (Figure 2A and Figure S5A). Germling fusion pairs of *erg-1* also showed membrane invaginations at the cell-to-cell contact zone similar to those observed in Δ*erg-10a*/Δ*erg-10b* (Figures S3A and S5B). For further analysis, we created a Δ*erg-1* gene knockout strain (Figure S5, C and D). Backcrossing of a primary transformant with WT revealed that the deletion of *erg-1* significantly delayed growth and development of the mutant progeny (Figure S6). Mycelia of Δ*erg-1* exhibited developmental defects similar to the classical *erg-1* mutant and the Δ*erg-10a*/Δ*erg-10b* isolate (Figure 2, A and B and Figure S5D). Consistent with the sterol composition reported for the classical *erg-1* mutant and an independent deletion strain (Grindle and Farrow 1978; Hu *et al.* 2018), our GC/MS analysis of Δ*erg-1* not only confirmed a block in ergosterol biosynthesis, but also the accumulation of mainly three sterol intermediates that all contained a double bond between positions C-8 and C-9, instead of C-7 and C-8, of the ring system (Figure 1A and Figure S7, A and B). Two of these intermediates (ergosta-8,22-dienol and fecosterol) also lacked the double bond between C-5 and C-6 (Figure S7B), comparable with the sterol accumulating in Δ*erg-10a*/Δ*erg-10b* (Figure 1B) (Weichert *et al.* 2016). In summary, mutations in the genes *erg-1* and *erg-10a*/*erg-10b* cause altered double bond arrangements in the B ring of the sterol core and result in comparable developmental defects.

While the frequency of interactions between Δ*erg-1* germlings (MW_308, 81.7 ± 0.9%) was comparable to WT (Weichert *et al.* 2016), cell pairs of this mutant typically formed membrane invaginations after physical contact reminiscent of Δ*erg-10a*/Δ*erg-10b*, Δ*Prm1*, and Δ*lfd-1* (Figure 4A and Figure S4A). Similar to Δ*erg-10a*/Δ*erg-10b*, the fusion frequency in Δ*erg-1* germlings was reduced by ~50% (Figure 4B). Knockout of the *Prm1* gene in Δ*erg-1* further reduced this number by another 50%, supporting the notion that the fusion defects caused by an altered sterol composition are independent of PRM1 (Figure 4B). While the triple mutant Δ*lfd-1*/Δ*erg-10a*/Δ*erg-10b* had also shown an additive fusion defect, the frequency of germling fusion in the Δ*lfd-1*/Δ*erg-1* double mutant (62%) was surprisingly in between those of the corresponding Δ*erg-1* (39%) and Δ*lfd-1* (87%) strains (Figure S4C). Although these observations show differences between both *erg* mutants with regard to LFD-1, their phenotypic similarities and additive fusion defects with Δ*Prm1* indicate that their altered sterol composition affects similar molecular processes. Since PRM1 and LFD-1 have independent and redundant roles during plasma membrane merger in *N. crassa* (Palma-Guerrero *et al.* 2014), both transmembrane proteins are probably differentially affected by an altered membrane composition. In conclusion, the structural similarities of the accumulating sterols in Δ*erg-10a*/Δ*erg-10b* and Δ*erg-1* (Figure 1B and Figure S7B) cause comparable

specific macroscopic and microscopic phenotypes, but appear to differentially impact membrane-associated proteins.

Membrane fusion in Δerg-10a/Δerg-10b and Δerg-1 is affected before engagement of the fusion machinery

Cells of *S. cerevisiae* and *N. crassa* lacking PRM1 homologs are prone to lysis during mating and germling fusion, respectively. Lysis correlates with cytoplasmic mixture, indicating that aberrant engagement of the fusion machinery results in membrane rupture and cell death (Jin *et al.* 2004; Aguilar *et al.* 2007). In both fungi, fusion-induced lysis is enhanced by low levels of extracellular calcium ions (Ca^{2+}), suggesting that Ca^{2+}-dependent repair mechanisms counteract this deficiency (Aguilar *et al.* 2007; Palma-Guerrero *et al.* 2014). Since germling pairs of Δ*erg-10a*/Δ*erg-10b* and Δ*erg-1* have a Δ*Prm1*-like defect in plasma membrane fusion (Figure 4A), we tested whether these *erg* mutants also undergo fusion-induced cell lysis. Consistent with previous reports (Palma-Guerrero *et al.* 2014), ∼12% of Δ*Prm1* cell pairs and 3% of WT pairings underwent lysis on regular MM (Figure 5). This frequency increased to ∼20% for Δ*Prm1* germling pairs when the Ca^{2+} content was reduced by one-half, compared with no significant increase in WT. In contrast to Δ*Prm1* and similar to WT, cell integrity of Δ*erg-10a*/Δ*erg-10b* and Δ*erg-1* fusion pairs was not compromised on regular medium, and only a slight increase in lysis was observed on reduced Ca^{2+}. Interestingly, introducing the deletion of *erg-10a/erg-10b* or *erg-1* into the Δ*Prm1* strain partially suppressed its lysis phenotype to a level of 8% on regular medium and 10% on reduced Ca^{2+} (Figure 5). Taken together, these data indicate that in the Δ*erg-10a*/Δ*erg-10b* and Δ*erg-1* mutants, membrane fusion is blocked at a stage before PRM1 is required and therefore before engagement of the fusion machinery.

In contrast to ΔPrm1, the deletion of erg genes only affects vegetative fusion but not mating

A major advantage of using *N. crassa* as a model system for studying cell-to-cell fusion is the occurrence of different experimentally amenable fusion events within its life cycle. These include vegetative fusion between genetically identical spore germlings, but also nonself sexual fusion between cells of different mating types (Fischer and Glass 2019). During sexual development of this heterothallic fungus, prefruiting bodies (protoperithecia) of the female partner form specialized receptive hyphae called trichogynes, which grow toward and fuse with pheromone-secreting male cells of the opposite mating type (Raju 1980; Bistis 1983).

The absence of PRM1 in *N. crassa* reduces successful cell-to-cell fusion in both vegetative and sexual cell merger by 50%, suggesting that the protein is part of a basic, general membrane fusion machinery (Fleissner *et al.* 2009b). Similarly, the *erg2* and *erg3* mutants of *S. cerevisiae* show significant reduced membrane fusion during mating (Jin *et al.* 2008). Based on the phenotypic similarity of Δ*Prm1* to Δ*erg-10a*/Δ*erg-10b* and Δ*erg-1* during germling fusion of *N. crassa* (Figure 4A), we hypothesized that mating might also

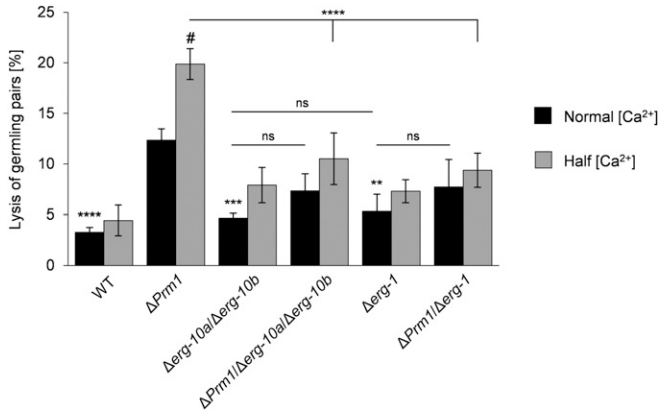

Figure 5 The various plasma membrane fusion mutants differ in the frequency of fusion-induced cell lysis. Quantitative analysis of cell lysis in germling pairs of WT (FGSC 2489) and mutants lacking *erg* genes and/or *Prm1* on MM, with normal and reduced levels of Ca^{2+}. Values represent the mean ± SD from three independent populations of 100–125 germling pairs per replicate, strain, and growth condition. Statistical analysis with ANOVA and Tukey's *post hoc* test: $^{**}P < 0.01$, $^{***}P < 0.001$, $^{****}P < 0.0001$ for comparisons with Δ*Prm1* at normal Ca^{2+} concentration; horizontal lines denote additional comparisons between strains ($^{***}P < 0.001$); # denotes a significant difference ($P < 0.001$) for comparisons of Δ*Prm1* between normal and half Ca^{2+} concentration, with no significant differences for any of the other strains between these two growth conditions. FGSC, Fungal Genetics Stock Center; MM, minimal medium; ns, not significant; WT, wild-type.

be affected in these *erg* mutants. To test this notion, protoperithecia of the *mat a* strain of WT or *erg* mutants were fertilized with uninuclear microconidia from *mat A* strains, whose nuclei were labeled by histone-1 (H1)-GFP (Figure 6A). Successful fusion of the mating partners resulted in transport of the male nucleus through the trichogyne and could be observed as disappearance of the GFP signal (Fleissner *et al.* 2009b). As a result, the Δ*erg-10a*/Δ*erg-10b* mutant was not impaired in sexual fusion, reaching trichogyne–microconidium fusion rates comparable with WT crosses (Figure 6, A and B). Since the Δ*erg-1* mutant formed only low numbers of protoperithecia (Figure S6, B and C), we could only analyze the impact of this gene deletion on male cells in heterozygous crosses with WT. Here too, no effect on mating fusion was observed (Figure 6B). Taken together, these data indicate that in *N. crassa*, the accumulation of membrane sterols with altered ring system structures specifically affects vegetative cell fusion (Figure 4B), but not mating fusion.

Based on these striking findings, we hypothesized that the sterol distributions in spore germlings and trichogynes might differ from each other. Staining with the sterol-binding dye filipin revealed sterol accumulation at the cell tips of spore germlings (Figure 7A), consistent with the occurrence of sterol-rich domains in the plasma membrane of various types of polarized fungal cells (Athanasopoulos *et al.* 2019). No differences in sterol distribution were observed among WT, Δ*erg-10a*/Δ*erg-10b*, and Δ*erg-1* germlings (Figure 7A). In

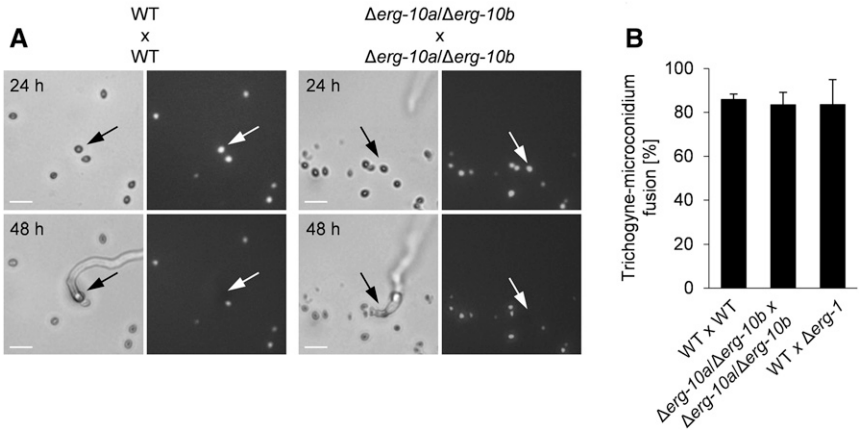

Figure 6 The deletion of *erg-10a/erg-10b* does not impact mating fusion in *N. crassa*. (A) Representative images of mating pairs in homozygous crossings of WT (FGSC 988 × N2-12) and Δ*erg-10a/*Δ*erg-10b* (N4-37 × MW_181). Microconidia (black arrows) expressing H1-GFP were observed before (24 hr) and after (48 hr) contact with a trichogyne of the opposite mating type (*mat a* × *mat A*). The disappearance of the nuclear fluorescence in the spores (white arrows) indicates cell-to-cell fusion events, resulting in the transition of nuclei via the trichogynes into the fruiting bodies. Bar, 10 μm. (B) Quantification of fusion between trichogynes and microconidia. Values represent the mean ± SD from three to six independent crossings for each combination with 39–122 mating pairs per replicate (no statistically significant differences were detected between these crosses: $P >> 0.05$, ANOVA with Dunnett's *post hoc* test). FGSC, Fungal Genetics Stock Center; WT, wild-type.

interacting WT germlings, both partner cells typically accumulated sterols at the plasma membrane while they were redirecting their growth toward each other (Figure 7B). While ~80% of interacting germ tubes possessed sterol-rich tips, sterol-rich membrane domains were remarkably almost absent in trichogynes growing toward a male cell (Figure 7, C and D). In contrast, an intense fluorescent signal was present along the entire plasma membrane of these receptive hyphae (Figure 7C). These data suggest fundamental differences in sterol distribution between vegetative and sexual cells of *N. crassa*.

Postfertilization events and fruiting body development are deficient in Δerg-10a/Δerg-10b and Δerg-1

Compared with yeast, the more complex sexual life cycle of *N. crassa* allows study of the impact of *erg* gene deletions during multicellular development, such as fruiting body formation (Raju 2009). Despite the normal mating fusion of Δ*erg-10a/*Δ*erg-10b* crossing partners (Figure 6), subsequent fruiting body development was strongly affected (Figure 8). In heterozygous crosses between WT as the female and Δ*erg-10a/*Δ*erg-10b* as the male partner, the number of mature asci and ascospores was moderately decreased compared with WT reference crosses. However, when Δ*erg-10a/*Δ*erg-10b* served as the female, fertility was strongly impaired, typically resulting in immature perithecia that harbored only a few or no asci, and produced barely any ascospores (Figure 8, A and B). To pinpoint this defect, we created a heterokaryon of the double mutant with the so-called *helper* strain (FGSC 4564) by vegetative fusion. The *helper* strain carries an inactive *MAT* locus and rescues only fertility defects that arise before karyogamy in the heterokaryotic perithecia (Perkins 1984). Using the Δ*erg-10a/*Δ*erg-10b/helper* heterokaryon as a female largely restored perithecial maturation and asci formation; however, only reduced numbers of ascospores were ejected (Figure 8, C and D). This observation indicates that the absence of *erg-10a* and *erg-10b* affects both pre- and postfertilization events in fruiting body development. Notably, the partially restored fertility of the Δ*erg-10a/*Δ*erg-10b/helper* heterokaryon phenocopied heterozygous crosses between the single mutants Δ*erg-10a* and Δ*erg-10b* (Figure S8A), which were originally pursued to construct the double knockout strain. While homozygous crosses between the single mutants were indistinguishable from the WT control, heterozygous crosses between Δ*erg-10a* and Δ*erg-10b* resulted in mature perithecia with full rosettes of asci that only produced limited amounts of black ascospores, which were not rescued in a heterokaryon with the *helper* strain (Figure S8, A and B). In the case of the heterozygous cross between Δ*erg-10a* and Δ*erg-10b*, one nucleus was WT for *erg-10a* and the other one for *erg-10b*. During meiosis, these genes cannot pair with their homologous copy because it is missing in the crossing partner. These mismatches within the pairs of homologous chromosomes result in MSUD (meiotic silencing of unpaired DNA), a temporary gene inactivation mechanism in *N. crassa* (Shiu *et al.* 2001). To test a potential role of MSUD in the observed fertility defects, we analyzed heterozygous crosses between Δ*erg-10a* and Δ*erg-10b* in which the male crossing partner carried a deletion of *Sad-1*, a gene that codes for an RNA-dependent RNA polymerase essential for MSUD (Shiu *et al.* 2001). Consistent with our hypothesis, Δ*Sad-1* fully restored the amount of mature ascospores in the asci of the heterozygous crosses between Δ*erg-10a* and Δ*erg-10b* (Figure S8C). By extending this approach to Δ*erg-10a/*Δ*erg-10b*, we observed that the combination of the *helper* strain and Δ*Sad-1* fully restored the fertility of the double mutant (Figure 8, C and D). These results indicate that MSUD contributes to the poor fertility of crosses involving the deletions Δ*erg-10a* and Δ*erg-10b* after karyogamy, probably by temporarily blocking ergosterol biosynthesis at the level of C-5 sterol desaturation within the developing asci.

Similar to Δ*erg-10a/*Δ*erg-10b*, the Δ*erg-1* mutant was also poorly fertile as the female crossing partner, which could only partially be rescued in a heterokaryon with the *helper* strain.

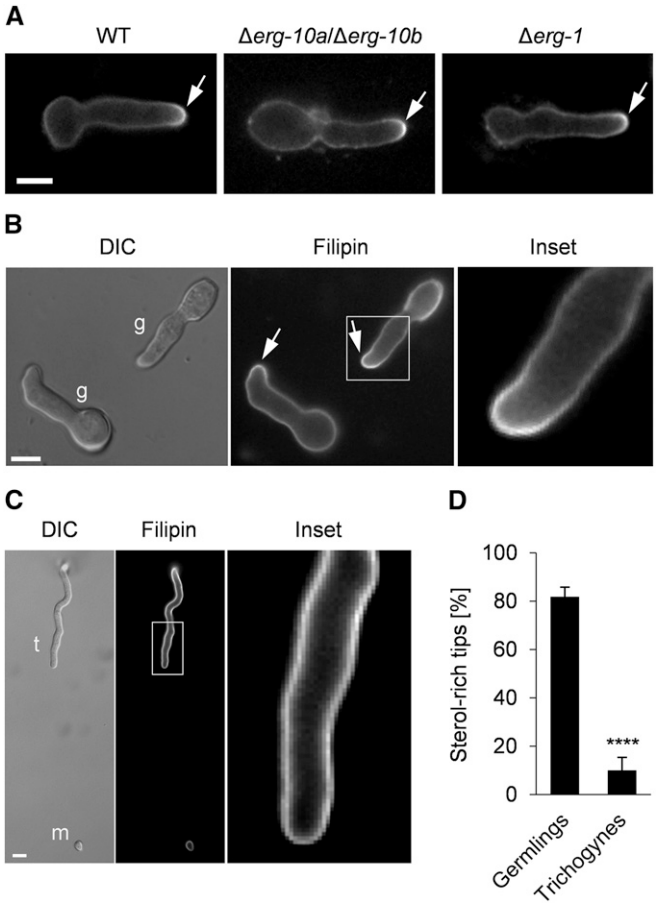

Figure 7 Membrane sterol distribution differs between vegetative and sexual cells of *N. crassa*. Germlings and trichogynes were stained with filipin. (A) Accumulation of sterols at the polarized cell tips of WT (FGSC 2489), Δ*erg-10a*/Δ*erg-10b* (N4-38), and Δ*erg-1* (MW_308) germlings. (B) Arrows indicate sterol-rich domains in interacting WT germlings (g). The white square marks the area of the enlarged image to the right. (C) Trichogyne (t)–microconidium (m) interaction. The white rectangle indicates the position of the enlarged image to the right. Bar in (A–C), 5 μm. (D) Quantification of sterol-rich cell tips in germlings and trichogynes during cell-to-cell interactions. Values represent the mean ± SD from three and two independent experiments with ∼100 germling pairs and up to 40 trichogynes per replicate (****$P < 0.0001$, unpaired, two-tailed Student's *t*-test). FGSC, Fungal Genetics Stock Center; WT, wild-type.

However, by introducing Δ*Sad-1* into these crosses, the fertility of Δ*erg-1* was completely restored (Figure S8D). Taken together, these results indicate that the accumulation of sterols with an altered double-bond arrangement in the ring system specifically impairs asci development and ascospore formation. Thus, the sterol composition in the membranes of diverse cell types involved in multicellular development differentially and specifically affects cellular behavior and function.

Discussion

Sterols are essential components of eukaryotic cell membranes and impact the properties of the lipid bilayer, as well as the function of membrane-associated proteins. In this study, we corroborate the hypothesis that specific structural sterol features have a distinct impact on specific cellular processes. While ergosterol precursors carrying a conjugated double bond in their aliphatic side chain, such as those accumulating in the Δ*erg-2* mutant, strongly affect cell-to-cell communication and cell contact recognition in germinating spores of *N. crassa* (Weichert *et al.* 2016), sterols with an altered ring system accumulating in the Δ*erg-10a*/Δ*erg-10b* and Δ*erg-1* mutants still promote these processes, but hinder subsequent plasma membrane merger. In a population of Δ*erg-10a*/Δ*erg-10b* or Δ*erg-1* spore germlings, about one-third of fusion pairs fail to merge, but two-thirds still undergo fusion. This indicates that the accumulating precursors can still support the fusion-related functions, but only to a limited extent. In addition, these B ring-modified sterol precursors are also generally able to support colony growth and development, but specifically affect the differentiation of vegetative spores and fruiting bodies. Notably, the marked drop in asexual sporulation of Δ*erg-10a*/Δ*erg-10b* and Δ*erg-1* as such (Figure 2B and Figure S5D) contrasts with normal conidiation of Δ*erg-2* and Δ*Prm1* cultures (Fleissner *et al.* 2009b; Weichert *et al.* 2016), suggesting that the cell fusion defects are independent of the deficiencies in colony differentiation.

The highly specific effect of sterol structure on cellular differentiation is particularly illustrated by the opposing outcomes in vegetative *vs.* sexual cell fusion in the Δ*erg-10a*/Δ*erg-10b* and Δ*erg-1* mutants. While plasma membrane merger during vegetative spore germling fusion is highly reduced, it is normal during sexual mating. The defect during vegetative fusion is strikingly similar to the phenotype of the Δ*Prm1* and Δ*lfd-1* mutants, which lack transmembrane proteins mediating plasma membrane fusion. Interestingly, however, the absence of these proteins affects vegetative and sexual fusion alike (Fleissner *et al.* 2009b; Palma-Guerrero *et al.* 2014), supporting the hypothesis that they are part of a general plasma membrane fusion machinery that mediates various fusion events within the fungal life cycle. However, so far our understanding of plasma membrane fusion in fungi remains extremely limited, in part because no fusogen has yet been identified in fungi (Aguilar *et al.* 2013). Normal fusion during mating of the Δ*erg-10a*/Δ*erg-10b* or Δ*erg*-1 strains indicates that the accumulation of the sterol precursors does not affect this proposed core fusion machinery, or its delivery to the plasma membrane, raising the question of where their deleterious effects come into play. A significant proportion of Δ*Prm1* or Δ*lfd-1* cell-to-cell pairs undergo lysis at the moment the fusion machinery is engaged. This observation has led to the notion that PRM1 and LFD-1 control the fidelity of the fusion process, probably by confining plasma membrane merger to a spatially restricted surface area (Aguilar *et al.* 2007; Palma-Guerrero *et al.* 2014). However, introduction of the Δ*erg-10a*/Δ*erg-10b* or Δ*erg-1* mutations into Δ*Prm1* or Δ*lfd-1* suppresses their lysis phenotype. Therefore, we hypothesize that in the *erg* mutants the block of the fusion process occurs before engagement of the fusion machinery, thereby making PRM1 and LFD-1 dispensable in those

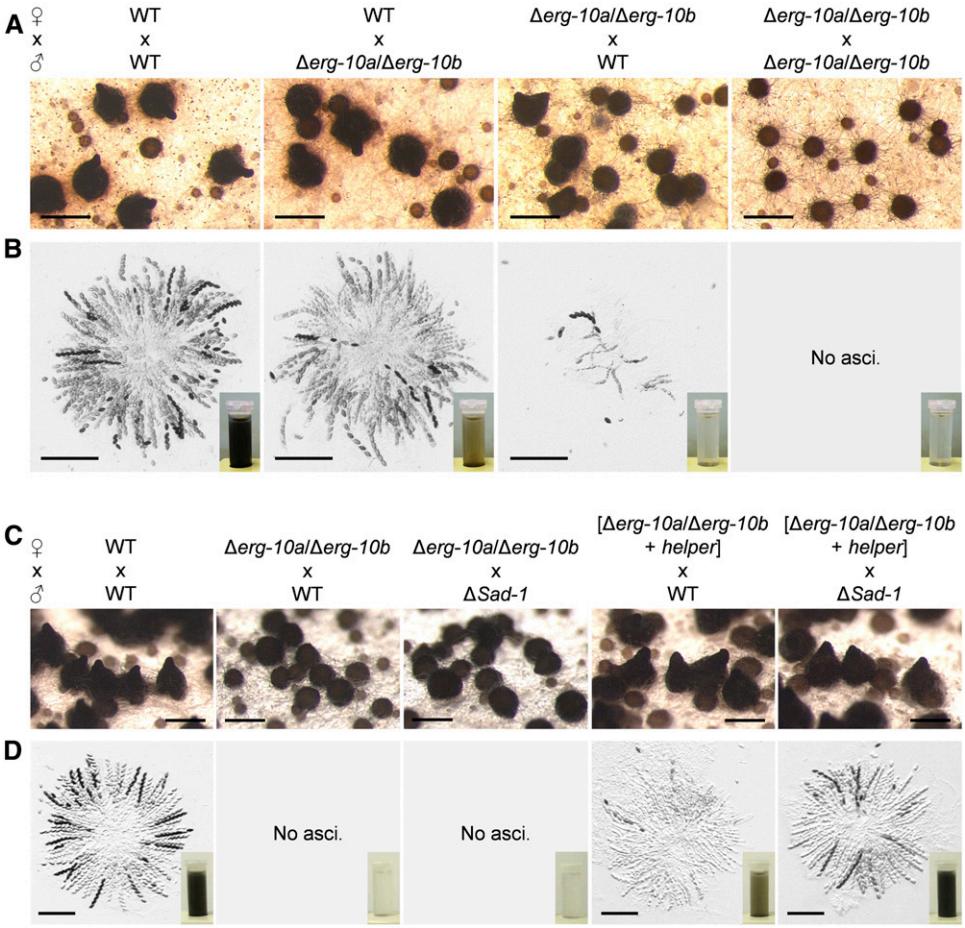

Figure 8 Fertility of the Δ*erg-10a*/Δ*erg-10b* mutant is affected by pre- and post-fertilization deficiencies. (A) Fruiting body development in homozygous and heterozygous crosses (*mat A* × *mat a*) of WT (FGSC 2489 and FGSC 988) and Δ*erg-10a*/Δ*erg-10b* (N4-38 and N4-37). (B) Microscopic analysis of rosettes of asci isolated from the fruiting bodies shown in (A). Inset images show the amount of ascospores harvested from one representative plate per crossing. (C and D) Analysis of perithecia, asci, and ascospores (insets) from crosses with a strain carrying the suppressor mutation Δ*Sad-1* (FGSC 11151) and/or involving the *helper* strain (FGSC 4564). Note that only the presence of the *helper* and the Δ*Sad-1* mutation fully restore fertility of the crosses. Bars in A and C, 500 μm; B and D, 200 μm. FGSC, Fungal Genetics Stock Center; WT, wild-type.

genetic backgrounds. So far, the molecular processes mediating the steps between cell-to-cell contact recognition and engagement of the fusion machinery remain elusive. Our data indicate that, even at these late stages of the fusion process, differences between vegetative and sexual fusion exist.

Vegetative and sexual cell-to-cell communication and fusion of filamentous fungi share core conserved factors with yeast mating. However, mounting evidence indicates that the homologs of these factors are differently wired during mating and germling fusion in *N. crassa*. While the upstream conserved pheromone receptors are only involved in trichogyne–conidium interactions, homologs of the downstream yeast pheromone response pathway are central for germling interaction in *N. crassa* and other molds (Daskalov *et al.* 2017; Fischer and Glass 2019). Surprisingly, several factors homologous to proteins involved in yeast mating are only essential for germling fusion but dispensable for mating of the mold, including the here analyzed ERG-10a/ERG-10b and ERG-1, but also ERG-2, the polarity factor BEM-1, or components of the striatin-interacting phosphatase and kinase (STRIPAK) signaling complex (Simonin *et al.* 2010; Schürg *et al.* 2012; Weichert *et al.* 2016). The role of the conserved pheromone response MAPKs in mating of *N. crassa* remains so far cryptic, since the respective mutants do not form prefruiting bodies or trichogynes (Maerz *et al.* 2008). However, the findings of this study support the hypothesis that mating of *S. cerevisiae* is mechanistically and evolutionarily more closely related to vegetative than sexual fusion of filamentous fungi. Together, these examples illustrate how conserved molecular building blocks have likely been recombined and repurposed during evolution.

Although mating fusion is unaffected in Δ*erg-10a*/Δ*erg-10b* or Δ*erg-1*, fruiting body formation and postfertilization events are deficient in these isolates. Partial complementation by the *helper* strain and rescue after inactivation of MSUD indicates independent effects of the altered sterol composition before and after karyogamy. Numerous cell fusion mutants are also affected in fruiting body formation, probably because cell-to-cell fusion contributes to the development of these multicellular structures (Lichius *et al.* 2012). Meiosis after karyogamy occurs in *N. crassa* in specialized cells, the so-called asci. Formation of each individual ascus also involves a cell-to-cell fusion event, the so-called crozier fusion, which could be hindered by the presence of the sterol precursors. However, testing of this hypothesis is cumbersome because these fusion events are not experimentally amenable. It will be of great interest to identify the molecular

functions and pathways specifically affected at various steps of the vegetative and sexual life cycle of the *erg* mutants.

While the molecular targets affected by the accumulation of the ergosterol precursors lacking a double bond at position C-5 or containing a C-8 desaturation (Figure 2 and Figure S7) remain elusive, their impact on membrane structure can be predicted. The structure of the sterol ring system determines the tilting angle of these molecules within the lipid bilayer and their interaction with other lipids (Róg *et al.* 2009; Mannock *et al.* 2010). As a consequence, alterations in this part of the sterols impair lipid packaging, and therefore fluidity and permeability of the membrane, as well as the formation of sterol-rich membrane domains. The sterol ring system also impacts membrane curvature, which is crucial for the fusion of lipid bilayers to surpass the high-energy barrier required for membrane merger, including vesicle fusion (Podbilewicz 2014; Yang *et al.* 2016). Similar to the germling fusion defects of Δ*erg-10a*/Δ*erg-10b* and Δ*erg-1* (Figure 4), the corresponding *erg3* and *erg2* mutants impaired in yeast mating also accumulate ergosterol precursors with an altered ring system (Heese-Peck *et al.* 2002; Jin *et al.* 2008). While the same plasma membrane fusion defect in another *S. cerevisiae* mutant, Δ*erg6*, has been attributed to the altered side-chain structure in the accumulating zymosterol (Jin *et al.* 2008), this sterol also features a double-bond arrangement in the ring system identical to fecosterol (Heese-Peck *et al.* 2002), one of the sterols accumulating in the absence of C-8 isomerase function (Figure 2B and Figure S7B). Therefore, we conclude that the ring system structure of sterols is a major determinant of plasma membrane fusion, possibly by impacting lipid–lipid interactions. In humans, the accumulation of 7-dehydrocholesterol, a precursor of cholesterol that contains one additional double bond at C-7 in the B ring, causes a severe developmental disorder known as Smith-Lemli-Opitz syndrome (Porter and Herman 2010). This sterol intermediate shows reduced interactions with the acyl chains of the phospholipids in the lipid bilayer, thereby reducing the order of the membranes and increasing the lateral mobility of the molecules within the lipid bilayer (Tulenko *et al.* 2006; Chen and Tripp 2012). Thus, structural alterations in sterols at the level of individual double bonds can have detrimental outcomes for cells, possibly paired with the depletion of the end product of sterol biosynthesis. However, the set of *erg* mutants available in *N. crassa* underscores that some sterol intermediates fully compensate for the loss of ergosterol (Weichert *et al.* 2016), highlighting that specific phenotypes caused by a block in sterol biosynthesis can exclusively correlate with the structure of the accumulating sterol species.

Acknowledgments

We are grateful to Louise Glass for sharing of *N. crassa* strains and Ralf Schnabel and Christian Hennig for continuous assistance in developing our microscopy. This work has been partially supported by funding from the German Research Foundation (Deutsche Forschungsgemeinschaft grant FL706/2-1 and FL706/3-1) to A.F.

Literature Cited

Aguilar, P. S., A. Engel, and P. Walter, 2007 The plasma membrane proteins Prm1 and Fig1 ascertain fidelity of membrane fusion during yeast mating. Mol. Biol. Cell 18: 547–556. https://doi.org/10.1091/mbc.e06-09-0776

Aguilar, P. S., M. G. Heiman, T. C. Walther, A. Engel, D. Schwudke *et al.*, 2010 Structure of sterol aliphatic chains affects yeast cell shape and cell fusion during mating. Proc. Natl. Acad. Sci. USA 107: 4170–4175. https://doi.org/10.1073/pnas.0914094107

Aguilar, P. S., M. K. Baylies, A. Fleissner, L. Helming, N. Inoue *et al.*, 2013 Genetic basis of cell-cell fusion mechanisms. Trends Genet. 29: 427–437. https://doi.org/10.1016/j.tig.2013.01.011

Athanasopoulos, A., B. André, V. Sophianopoulou, and C. Gournas, 2019 Fungal plasma membrane domains. FEMS Microbiol. Rev. 43: 642–673. https://doi.org/doi: 10.1093/femsre/fuz022

Bistis, G. N., 1981 Chemotropic interactions between trichogynes and conidia of opposite mating-type in *Neurospora crassa*. Mycologia 73: 959–975. https://doi.org/10.1080/00275514.1981.12021425

Bistis, G. N., 1983 Evidence for diffusible, mating-type-specific trichogyne attractants in *Neurospora crassa*. Exp. Mycol. 7: 292–295. https://doi.org/10.1016/0147-5975(83)90051-8

Chen, C., and C. P. Tripp, 2012 A comparison of the behavior of cholesterol, 7-dehydrocholesterol and ergosterol in phospholipid membranes. Biochim. Biophys. Acta Biomembr. 1818: 1673–1681. https://doi.org/10.1016/j.bbamem.2012.03.009

Christianson, T. W., R. S. Sikorski, M. Dante, J. H. Shero, and P. Hieter, 1992 Multifunctional yeast high-copy-number shuttle vectors. Gene 110: 119–122. https://doi.org/10.1016/0378-1119(92)90454-W

Colot, H. V., G. Park, G. E. Turner, C. Ringelberg, C. M. Crew *et al.*, 2006 A high-throughput gene knockout procedure for *Neurospora* reveals functions for multiple transcription factors. Proc. Natl. Acad. Sci. USA 103: 10352–10357 (erratum: Proc. Natl. Acad. Sci. USA 103: 16614). https://doi.org/10.1073/pnas.0601456103

Curto, M.-A., M. R. Sharifmoghadam, E. Calpena, N. De Leon, M. Hoya *et al.*, 2014 Membrane organization and cell fusion during mating in fission yeast requires multipass membrane protein Prm1. Genetics 196: 1059–1076. https://doi.org/10.1534/genetics.113.159558

Daskalov, A., J. Heller, S. Herzog, A. Fleißner, and N. L. Glass, 2017 Molecular mechanisms regulating cell fusion and heterokaryon formation in filamentous fungi, pp. 215–229 in *The Fungal Kingdom*, edited by J. Heitman, B. Howlett, P. Crous, E. Stukenbrock, T. James, *et al.* American Society of Microbiology (ASM), Washington, DC.

Dufourc, E. J., 2008 Sterols and membrane dynamics. J. Chem. Biol. 1: 63–77. https://doi.org/10.1007/s12154-008-0010-6

Fischer, M. S., and N. L. Glass, 2019 Communicate and fuse: how filamentous fungi establish and maintain an interconnected mycelial network. Front. Microbiol. 10: 619. https://doi.org/10.3389/fmicb.2019.00619

Fleissner, A., and N. L. Glass, 2007 SO, a protein involved in hyphal fusion in *Neurospora crassa*, localizes to septal plugs. Eukaryot. Cell 6: 84–94. https://doi.org/10.1128/EC.00268-06

Fleissner, A., S. Sarkar, D. J. Jacobson, M. G. Roca, N. D. Read *et al.*, 2005 The so locus is required for vegetative cell fusion and postfertilization events in *Neurospora crassa*. Eukaryot. Cell 4: 920–930. https://doi.org/10.1128/EC.4.5.920-930.2005

Fleissner, A., A. C. Leeder, M. G. Roca, N. D. Read, and N. L. Glass, 2009a Oscillatory recruitment of signaling proteins to cell tips promotes coordinated behavior during cell fusion. Proc. Natl.

Acad. Sci. USA 106: 19387–19392. https://doi.org/10.1073/pnas.0907039106

Fleissner, A., S. Diamond, and N. L. Glass, 2009b The *Saccharomyces cerevisiae* PRM1 homolog in *Neurospora crassa* is involved in vegetative and sexual cell fusion events but also has postfertilization functions. Genetics 181: 497–510. https://doi.org/10.1534/genetics.108.096149

Fleißner, A., and S. Herzog, 2016 Signal exchange and integration during self-fusion in filamentous fungi. Semin. Cell Dev. Biol. 57: 76–83. https://doi.org/10.1016/j.semcdb.2016.03.016

Freitag, M., and E. U. Selker, 2005 Expression and visualization of red fluorescent protein (RFP) in *Neurospora crassa*. Fungal Genet. Newsl. 52: 14–17. https://doi.org/10.4148/1941-4765.1124

Freitag, M., P. C. Hickey, N. B. Raju, E. U. Selker, and N. D. Read, 2004 GFP as a tool to analyze the organization, dynamics and function of nuclei and microtubules in *Neurospora crassa*. Fungal Genet. Biol. 41: 897–910. https://doi.org/10.1016/j.fgb.2004.06.008

Grindle, M., 1973 Sterol mutants of *Neurospora crassa*: their isolation, growth characteristics and resistance to polyene antibiotics. Mol. Gen. Genet. 120: 283–290. https://doi.org/10.1007/BF00267158

Grindle, M., 1974 The efficacy of various mutagens and polyene antibiotics for the induction and isolation of sterol mutants of *Neurospora crassa*. Mol. Gen. Genet. 130: 81–90. https://doi.org/10.1007/BF00270520

Grindle, M., and R. Farrow, 1978 Sterol content and enzyme defects of nystatin-resistant mutants of *Neurospora crassa*. Mol. Gen. Genet. 165: 305–308. https://doi.org/10.1007/BF00332531

Heese-Peck, A., H. Pichler, B. Zanolari, R. Watanabe, G. Daum *et al*., 2002 Multiple functions of sterols in yeast endocytosis. Mol. Biol. Cell 13: 2664–2680. https://doi.org/10.1091/mbc.e02-04-0186

Heiman, M. G., and P. Walter, 2000 Prm1p, a pheromone-regulated multispanning membrane protein, facilitates plasma membrane fusion during yeast mating. J. Cell Biol. 151: 719–730. https://doi.org/10.1083/jcb.151.3.719

Herzog, S., M. R. Schumann, and A. Fleißner, 2015 Cell fusion in *Neurospora crassa*. Curr. Opin. Microbiol. 28: 53–59. https://doi.org/10.1016/j.mib.2015.08.002

Herzog, S., H. Brinkmann, M. Vences, and A. Fleißner, 2020 Evidence of repeated horizontal transfer of sterol C-5 desaturase encoding genes among dikarya fungi. Mol. Phylogenet. Evol. 150: 106850. https://doi.org/10.1016/j.ympev.2020.106850

Hickey, P. C., D. J. Jacobson, N. D. Read, and N. L. Glass, 2002 Live-cell imaging of vegetative hyphal fusion in *Neurospora crassa*. Fungal Genet. Biol. 37: 109–119. https://doi.org/10.1016/S1087-1845(02)00035-X

Hu, C., M. Zhou, W. Wang, X. Sun, O. Yarden *et al*., 2018 Abnormal ergosterol biosynthesis activates transcriptional responses to antifungal azoles. Front. Microbiol. 9: 9. https://doi.org/10.3389/fmicb.2018.00009

Jin, H., C. Carlile, S. Nolan, and E. Grote, 2004 Prm1 prevents contact-dependent lysis of yeast mating pairs. Eukaryot. Cell 3: 1664–1673. https://doi.org/10.1128/EC.3.6.1664-1673.2004

Jin, H., J. M. McCaffery, and E. Grote, 2008 Ergosterol promotes pheromone signaling and plasma membrane fusion in mating yeast. J. Cell Biol. 180: 813–826. https://doi.org/10.1083/jcb.200705076

Lichius, A., K. M. Lord, C. E. Jeffree, R. Oborny, P. Boonyarungsrit *et al*., 2012 Importance of MAP kinases during protoperithecial morphogenesis in *Neurospora crassa*. PLoS One 7: e42565. https://doi.org/10.1371/journal.pone.0042565

Maerz, S., C. Ziv, N. Vogt, K. Helmstaedt, N. Cohen *et al*., 2008 The nuclear Dbf2-related kinase COT1 and the mitogen-activated protein kinases MAK1 and MAK2 genetically interact to regulate filamentous growth, hyphal fusion and sexual development in *Neurospora crassa*. Genetics 179: 1313–1325. https://doi.org/10.1534/genetics.108.089425

Mannock, D. A., R. N. A. H. Lewis, T. P. W. McMullen, and R. N. McElhaney, 2010 The effect of variations in phospholipid and sterol structure on the nature of lipid-sterol interactions in lipid bilayer model membranes. Chem. Phys. Lipids 163: 403–448. https://doi.org/10.1016/j.chemphyslip.2010.03.011

Margolin, B. S., M. Freitag, and E. U. Selker, 1997 Improved plasmids for gene targeting at the *his-3* locus of *Neurospora crassa* by electroporation. Fungal Genet. Newsl. 44: 34–36. https://doi.org/10.4148/1941-4765.1281

Nawrath, T., J. S. Dickschat, B. Kunze, and S. Schulz, 2010 The biosynthesis of branched dialkylpyrazines in myxobacteria. Chem. Biodivers. 7: 2129–2144. https://doi.org/10.1002/cbdv.201000158

Palma-Guerrero, J., A. C. Leeder, J. Welch, and N. L. Glass, 2014 Identification and characterization of LFD1, a novel protein involved in membrane merger during cell fusion in *Neurospora crassa*. Mol. Microbiol. 92: 164–182. https://doi.org/10.1111/mmi.12545

Perkins, D., 1984 Advantages of using the inactive-mating-type *am1* strain as a helper component in heterokaryons. Fungal Genet. Newsl. 31: 41–42.

Podbilewicz, B., 2014 Virus and cell fusion mechanisms. Annu. Rev. Cell Dev. Biol. 30: 111–139. https://doi.org/10.1146/annurev-cellbio-101512-122422

Porter, F. D., and G. E. Herman, 2010 Malformation syndromes caused by disorders of cholesterol synthesis. J. Lipid Res. 52: 6–34. https://doi.org/10.1194/jlr.R009548

Raju, N. B., 1980 Meiosis and ascospore genesis in *Neurospora*. Eur. J. Cell Biol. 23: 208–223.

Raju, N. B., 2009 *Neurospora* as a model fungus for studies in cytogenetics and sexual biology at Stanford. J. Biosci. 34: 139–159. https://doi.org/10.1007/s12038-009-0015-5

Raymond, C. K., T. A. Pownder, and S. L. Sexson, 1999 General method for plasmid construction using homologous recombination. Biotechniques 26: 134–141. https://doi.org/10.2144/99261rr02

Richard, F., N. L. Glass, and A. Pringle, 2012 Cooperation among germinating spores facilitates the growth of the fungus, *Neurospora crassa*. Biol. Lett. 8: 419–422. https://doi.org/10.1098/rsbl.2011.1141

Roca, M. G., N. D. Read, and A. E. Wheals, 2005 Conidial anastomosis tubes in filamentous fungi. FEMS Microbiol. Lett. 249: 191–198. https://doi.org/10.1016/j.femsle.2005.06.048

Róg, T., M. Pasenkiewicz-Gierula, I. Vattulainen, and M. Karttunen, 2009 Ordering effects of cholesterol and its analogues. Biochim. Biophys. Acta 1788: 97–121. https://doi.org/10.1016/j.bbamem.2008.08.022

Schumann, M. R., U. Brandt, C. Adis, L. Hartung, and A. Fleißner, 2019 Plasma membrane integrity during cell-cell fusion and in response to pore-forming drugs is promoted by the penta-EF-hand protein PEF1 in *Neurospora crassa*. Genetics 213: 195–211. https://doi.org/10.1534/genetics.119.302363

Schürg, T., U. Brandt, C. Adis, and A. Fleissner, 2012 The *Saccharomyces cerevisiae* BEM1 homologue in *Neurospora crassa* promotes co-ordinated cell behaviour resulting in cell fusion. Mol. Microbiol. 86: 349–366. https://doi.org/10.1111/j.1365-2958.2012.08197.x

Serrano, A., J. Illgen, U. Brandt, N. Thieme, A. Letz *et al*., 2018 Spatio-temporal MAPK dynamics mediate cell behavior coordination during fungal somatic cell fusion. J. Cell Sci. 131: jcs213462. https://doi.org/10.1242/jcs.213462

Shiu, P. K., N. B. Raju, D. Zickler, and R. L. Metzenberg, 2001 Meiotic silencing by unpaired DNA. Cell 107: 905–916. https://doi.org/10.1016/S0092-8674(01)00609-2

Simonin, A. R., C. G. Rasmussen, M. Yang, and N. L. Glass, 2010 Genes encoding a striatin-like protein (*ham-3*) and a forkhead associated protein (*ham-4*) are required for hyphal fusion in *Neurospora crassa*. Fungal Genet. Biol. 47: 855–868. https://doi.org/10.1016/j.fgb.2010.06.010

Staben, C., B. Jensen, M. Singer, J. Pollock, M. Schechtman *et al.*, 1989 Use of a bacterial Hygromycin B resistance gene as a dominant selectable marker in *Neurospora crassa* transformation. Fungal Genet. Newsl. 36: 79–81. https://doi.org/10.4148/1941-4765.1519

Tatum, E. L., R. W. Barratt, and V. M. Cutter, 1949 Chemical induction of colonial paramorphs in *Neurospora* and *Syncephalastrum*. Science 109: 509–511. https://doi.org/10.1126/science.109.2838.509

Tulenko, T. N., K. Boeze-Battaglia, R. P. Mason, G. S. Tint, R. D. Steiner *et al.*, 2006 A membrane defect in the pathogenesis of the Smith-Lemli-Opitz syndrome. J. Lipid Res. 47: 134–143. https://doi.org/10.1194/jlr.M500306-JLR200

Vogel, H. J., 1956 A convenient growth medium for *Neurospora*. Microb. Genet. Bull. 13: 42–46.

Weichert, M., A. Lichius, B.-E. Priegnitz, U. Brandt, J. Gottschalk *et al.*, 2016 Accumulation of specific sterol precursors targets a MAP kinase cascade mediating cell–cell recognition and fusion. Proc. Natl. Acad. Sci. USA 113: 11877–11882. https://doi.org/10.1073/pnas.1610527113

Westergaard, M., and H. K. Mitchell, 1947 Neurospora V. A synthetic medium favoring sexual reproduction. Am. J. Bot. 34: 573–577. https://doi.org/10.1002/j.1537-2197.1947.tb13032.x

Winston, F., C. Dollard, and S. L. Ricupero-Hovasse, 1995 Construction of a set of convenient *Saccharomyces cerevisiae* strains that are isogenic to S288C. Yeast 11: 53–55. https://doi.org/10.1002/yea.320110107

Yang, S.-T., A. J. B. Kreutzberger, J. Lee, V. Kiessling, and L. K. Tamm, 2016 The role of cholesterol in membrane fusion. Chem. Phys. Lipids 199: 136–143. https://doi.org/10.1016/j.chemphyslip.2016.05.003

Communicating editor: M. Freitag